Evaporation–Wind Feedback and Low-Frequency Variability in the Tropical Atmosphere

J. DAVID NEELIN

Geophysical Fluid Dynamics Program, Princeton University, Princeton, NJ 08542

ISAAC M. HELD AND KERRY H. COOK

Geophysical Fluid Dynamics Laboratory/NOAA, Princeton University, Princeton, NJ 08542

(Manuscript received 18 December 1986, in final form 23 March 1987)

ABSTRACT

A mechanism by which feedback between zonal wind perturbations and evaporation can create unstable, low-frequency modes in a simple two-layer model of the tropical troposphere is presented. The modes resemble the 30–50 day oscillation. A series of general circulation model experiments designed to test the effect of suppressing this feedback on low-frequency variability in the model tropics is described. The results suggest that the evaporation–wind feedback can be important to the amplitude of the spectral peak corresponding to the 30–50 day oscillation in the model, but that the existence of the oscillation does not depend on it. The feedback is found to have a much more dramatic effect on low-frequency variability when sea surface temperatures are fixed than when the lower boundary is a zero heat capacity "swamp".

1. Introduction

There is a large amount of intraseasonal variability at large zonal scales in the tropical atmosphere. A prominent feature of this variability is the 30–50 day oscillation discovered by Madden and Julian (1971, 1972) which has been observed throughout the year in such fields as zonal wind, surface pressure, velocity potential and outgoing longwave radiation. It is dominated, at least in the wind and pressure fields, by eastward-moving zonal wavenumber 1 and 2 components (e.g., Maruyama, 1982; Lorenc, 1984; Krishnamurti et al., 1985; Murakami and Nakazawa, 1985; Lau and Chan, 1985). Recently, oscillations that resemble these observations in several respects have been diagnosed in a GCM with realistic geography (Lau and Lau, 1986; Hayashi and Golder, 1986) and in GCMs with zonally symmetric climates (Hayashi and Sumi, 1986; Palmer, 1986, personal communication).

No explanation for this phenomenon is generally accepted, although a number have been proposed, including free equatorial Kelvin waves in a dissipative atmosphere, wave-CISK and ground hydrological cycle mechanisms (e.g., Chang, 1977; Yamagata and Hayashi, 1984; Lindzen, 1974; Lau and Peng, 1987; Webster, 1983). Zonally symmetric oscillations on this time scale have been discussed by Stevens (1983) and Goswami and Shukla (1984). The purpose of this paper is to add another mechanism to this list, and to test it in a series of GCM experiments. The mechanism involves feedback between zonal wind perturbations and evaporation. Specifically, a region of anomalous latent heating on the equator will force anomalous easterly winds to the east of the region and westerlies to the west at low levels. If these perturbation winds are superposed on mean easterlies, as in the tropics, the strength of the surface zonal winds will increase to the east of the heating and decrease to the west. Because it depends on wind speed, evaporation will also increase to the east and decrease to the west. The resulting evaporation anomaly will then feed back onto the latent heating anomaly. Under certain assumptions the heating anomaly will be strengthened to the east and weakened to the west. The resulting feedback can favor or create eastward-propagating modes. A virtually identical mechanism is independently considered by Emanuel (1987).

We examine this mechanism in the context of a simple two-layer model in section 2, and discuss its destabilizing effect on certain modes of the system in section 3. In section 4, we proceed to test the effects of the mechanism on the low-frequency variability of a GCM. The GCM experiments are performed using idealized, zonally symmetric boundary conditions. A comparison is also made of the low-frequency variability in experiments with fixed sea surface temperature (SST) and moist continent ("swamp") boundary conditions.

2. A simple model with evaporation-wind feedback

Our starting point is a two-layer model, linearized about a barotropic zonal flow, $\bar{u}$, on an equatorial beta plane

$$(\partial_t + \bar{u}\partial_x + K_m)u_i - fv_i + \partial_x\phi_i = 0 \quad (1)$$

$$(\partial_t + \bar{u}\partial_x + K_m)v_i + fu_i + \partial_y \phi_i = 0 \quad (2)$$

$$(\partial_t + \bar{u}\partial_x + K_T)C_pT - \Delta s(\partial_x u_2 + \partial_y v_2) = (\Delta p/g)^{-1}LP \quad (3)$$

$$(\phi_1 - \phi_2)/2 = BT \quad (4)$$

$$(\partial_x u_1 + \partial_y v_1) = -(\partial_x u_2 + \partial_y v_2). \quad (5)$$

The subscripts $i = 1, 2$ refer to upper and lower layers, respectively; T is a midtropospheric temperature perturbation, P the precipitation, Δs the dry static energy difference between layers, Δp the pressure depth of the troposphere, $B = R/2$ where R is the gas constant, C_p the heat capacity of air at constant pressure, and L the latent heat of condensation. The constants K_m and K_T are the coefficients of Raleigh friction and Newtonian cooling.

Following Matsuno (1966) and Gill (1980), we construct the simplest possible model of the tropics by choosing the same friction coefficient, K_m, in each layer and taking $\bar{u}$ constant in height so that heating forces only the baroclinic mode, with $\phi_1 = -\phi_2 = BT$, etc. Friction in the lower layer can be thought of as due to turbulent exchange of momentum with the surface. In a separate study, we find that a value of (2 days)$^{-1}$ is suitable for simulating a GCM's low-level response to heating anomalies with the model (1)–(5). It is difficult to justify such a large value in the upper layer, although momentum mixing associated with moist convection likely provides some damping of the vertical shear (e.g., Sui and Yanai, 1986). In light of such uncertainties, we take (2–5 days)$^{-1}$ as an appropriate range of values for the mechanical damping. It should be noted that for steady, forced motions, as in Gill (1980), the term involving C_pT in (3) is negligible (except for the zonally symmetric component) and the system (1)–(3) may be solved for the lower-layer flow without reference to the upper layer. However, this is not true in the present application, so we expect that the poor treatment of the upper layer damping is a more significant problem here.

We add to these equations a vertically integrated moisture budget in which horizontal gradients of moisture are assumed sufficiently small that the term $\mathbf{V} \cdot \nabla q$ is negligible relative to $q\nabla \cdot \mathbf{V}$ and in which storage and horizontal transport of moisture in the upper layer is neglected:

$$\partial_t q + q(\partial_x u_2 + \partial_y v_2) = (E - P)(g/\Delta p). \quad (6)$$

Here q is the specific humidity in the lower layer and E is the evaporation. A specification of P is required to close the system. The simplest method is to prevent q from rising above a saturation value $\bar{q}$ by raining out the excess moisture. We make the further simplifying assumption that, averaged over the time scales of interest, it is always raining everywhere in the tropics, so that $q = \bar{q}$ and (6) becomes

$$\bar{q}(\partial_x u_2 + \partial_y v_2) = (E - P)(g/\Delta p). \quad (7)$$

Quantities without overbars now refer to deviations from the basic state. We can combine (3) and (7) to form the moist static energy budget of the perturbation

$$(\partial_t + \bar{u}\partial_x + K_T)C_pT - \Delta m(\partial_x u_2 + \partial_y v_2) = \mathrm{LE}(g/\Delta p), \quad (8)$$

where $\Delta m = \Delta s - L\bar{q}$ is the moist static energy difference between the two layers. Radiational and sensible heating contributions to the perturbation budget have been neglected, aside from the Newtonian cooling term. This seems adequate for a fixed surface temperature lower boundary but would not be correct over a continental surface. As a result, we think of the following derivation of the evaporation-wind feedback as applying *only to the fixed SST case.* We have also neglected possible variations in $\bar{q}$ due to perturbation temperature variations, but these would only change the effective value of B in (4). Perhaps more serious is our neglect of variations in q that would occur in a more flexible parameterization of P. The variations in q associated with the 30–50 day oscillation are undoubtedly small compared to the climatological values of q, but terms that are small in the moisture budget need not be negligible in the moist static energy budget; in particular, small changes in q could result in significant changes in Δm.

Evaporation is parameterized as

$$E_{\mathrm{total}} = \rho C_D |\mathbf{V}|(q_* - q) \quad (9)$$

where q_* is the saturation mixing ratio at the ground. If we assume that the low-level wind consists of the mean zonal flow, $\bar{u}$, plus a small zonal perturbation, u, the evaporative perturbation will be approximately

$$E = -A^*u \quad (10)$$

where the sign of A^* depends on the sign of $\bar{u}$ and has been chosen such that A^* is positive when $\bar{u}$ is easterly. Once again, we have neglected possible variations in $\bar{q}$ associated with changes in T, but these would simply act as an additional thermal damping in (8) and could be combined with K_T. Anomalies in evaporation can clearly be seen in composites of the analog to the 30–50 day oscillation in the GCM (N. C. Lau and T. Knutson, personal communication). These suggest a value of A^* of about 0.2 mm day^{-1} (m s^{-1})$^{-1}$ [equivalent to 0.05 K day^{-1} (m s^{-1})$^{-1}$ heating distributed through the troposphere]. If one simply linearizes (9) using values estimated from the GCM climatology, one obtains a value of A^* about four times as large. A small part of this difference is due to the fact that the composited anomaly winds are not parallel or antiparallel to the mean winds. More importantly, the variation in wind *speed* on the time scale of the 30–50 day oscillation is dependent not only on the wind variations on this time scale and on the climatological mean wind but also on higher frequency eddies. These higher frequency motions have the effect of reducing the variation in wind speed on the time scale of the 30–50 day oscillation for a given variation in wind on this time scale, effectively reducing A^*. This dependence of A^* on the "noise" level in the tropics is an interesting complication, but should not affect the gross features of the mechanism.

We thus have a shallow water system with a moist static stability, and with an evaporation feedback term in the moist static energy equation. In terms of lower layer perturbations, u, v and ϕ, we have

$$(\partial_t + \bar{u}\partial_x + K_m)u - fv + \partial_x\phi = 0 \quad (11a)$$

$$(\partial_t + \bar{u}\partial_x + K_m)v + fu + \partial_y\phi = 0 \quad (11b)$$

$$(\partial_t + \bar{u}\partial_x + K_T)\phi + c_0^2(\partial_x u + \partial_y v) = Au \quad (11c)$$

where $c_0^2 = \Delta mB/C_p$ and where A^* has been rescaled as

$$A = (g/\Delta p)(LBA^*/C_p) \approx 7 \text{ m s}^{-1}/\text{day}. \quad (12)$$

With the exception of the term involving c_0^2, this system is identical to the one employed by Emanuel (1987), although the interpretations given to some of the terms and the estimates of the coefficients differ.

3. Modes of the system

Assuming a form $\exp\{ik[x - (c + \bar{u})t]\}$ for the perturbations, we first examine the $v = 0$ mode of system (11). The dispersion relation is

$$kc = -i(K_m + K_T)/2 \pm [c_0^2k^2 + ikA - (K_m - K_T)^2/4]^{1/2} \quad (13)$$

where c is the Doppler-shifted phase speed. One of the modes can be eliminated by requiring the perturbation to decay at large y. To satisfy this condition, one must choose the sign which yields a positive real part to the phase speed.

The dispersion relation (13) contains two mechanisms which can give eastward propagation: one involving the term in c_0^2 and the other due to the evaporation-wind feedback coefficient A. For $A = 0$, one recovers the familiar damped Kelvin wave, but with a moist rather than dry static stability appearing in the phase speed c_0. In the opposite limit, we can consider the case where $\Delta m = 0$, giving $c_0^2 = 0$, in order to examine the effects of the evaporation–wind feedback in isolation. Since we expect Δm to be much smaller than Δs, certain properties of the wave in this limiting case turn out to be similar to those found using a nonzero value for Δm of plausible magnitude. Taking $\Delta m = 0$ is equivalent to assuming that the atmosphere is moist neutrally stable in the sense that, averaged over the troposphere, latent heating due to moisture convergence is exactly balanced by adiabatic cooling due to ascent. We simplify further by assuming that the thermal damping time, K_T^{-1}, is much longer than the frictional damping time, K_m^{-1}. The resulting dispersion relation in the $\Delta m = 0$ limit is

$$kc = -iK_m/2 + i(K_m^2/4 - ikA)^{1/2} \quad (14)$$

where the sign has been chosen to satisfy the y boundary conditions for $A > 0$ (basic state easterlies).

For the value of A in (12), and the range of values of K_m suggested above, (2–5 days)$^{-1}$, (14) gives a period of 38 to 30 days for wavenumber 1, and 23 to 20 days for wavenumber 2. The corresponding phase speed ranges are 12–15 m s^{-1} for wavenumber 1, and 10–11 m s^{-1} for wavenumber 2. The growth rate for wavenumber 1 ranges from (20 days)$^{-1}$ to (7 days)$^{-1}$, and for wavenumber 2 from (9 days)$^{-1}$ to (5 days)$^{-1}$. The growth rates in particular are quite sensitive to the values of K_m and A.

The meridional structure of the mode is of the form $\exp[-y^2/(2L^2)]$, where

$$L^{-2} = \beta(c_R - ic_I')/(c_R^2 + c_I'^2),$$

$$c_I' = c_I + K_m/k \quad \text{and} \quad c = c_R + ic_I. \quad (15)$$

The L^{-2} has a positive real part which causes the mode to decay in y: For K_m = (2 days)$^{-1}$, the decay scale is 40° latitude. Weaker damping produces a narrower mode; K_m = (5 days)$^{-1}$ results in a decay scale of 15° latitude. There is also an oscillatory component, but the first zero does not occur until y = 43°–38° latitude for this range of K_m. One cannot take this meridional structure very seriously if the predicted width is more than 10° or so, based as it is on the assumptions that the basic state is at rest and that the atmosphere is everywhere "saturated".

An interesting limit of (14) is $K_m^2 \gg kA$, although this is not really justified for the parameter estimates under consideration: $kA \approx$ (10 days)$^{-2}$ for wavenumber 1. For small kA/K_m^2, one obtains

$$c = A/K_m + ikA^2/K_m^3 + O(k^2A^3/K_m^5). \quad (16)$$

We find in this limit that the phase speed is independent of k. The fast decay terms of order K_m have cancelled. In fact, slow growth occurs despite arbitrarily large mechanical damping. For $A < 0$ (basic state westerlies), on the other hand, the admissible mode would decay rapidly.

The characteristics of this eastward-propagating, equatorially trapped mode are suggestive of the 30–50 day oscillation, although the growth rates do not yield a selectivity for the largest scales. The growth rates predicted by (13) asymptote to a constant as k becomes large so long as $\Delta m \neq 0$ [it is (13) rather than (14) which is relevant in the large k limit because the $c_0^2k^2$ term becomes important at large k even for very small c_0]. At least the growth rate does not go to infinity as the scale becomes small. Some scale selectivity in the damping mechanism could remove the smaller scales but it is more tempting to argue, as for many other problems of geophysical interest, that there is not a simple connection between linear theory growth rates and the statistically steady spectrum. In any case, the similarity to the 30–50 day oscillation seems sufficient to motivate the GCM experiments presented in section 4.

In the mode governed by (13), the evaporation–wind feedback coexists with a second mechanism for obtaining low-frequency, eastward-propagating waves, namely the moist static stability. This Δm is expected to be much smaller than the dry static stability, Δs; Neelin and Held (1987) have some success in simulating the tropical convergence zones using values of $\Delta m \approx 0.1\Delta s$ in regions of greatest low-level moisture. This would give "moist Kelvin wave" speeds about one third of the dry phase speed, placing them at about 20 m s^{-1} if a typical value of the dry phase speed is 60 m s^{-1} (taking $\Delta s/C_p = 25$ K). Although the appearance of a constant moist stability in this model is dependent on several assumptions, including linearization about a basic state which is everywhere precipitating, and on the simple vertical structure of the two-layer model, we suspect that its gross characteristics carry over to more realistic model atmospheres. There is some similarity to the stable "CISK" mechanism discussed by Lau and Peng (1987).

When both nonzero moist static stability and the evaporation–wind feedback mechanism are present together, (13) indicates that the hybrid mode will have a phase speed slightly higher than that obtained from either mechanism alone, and a growth rate on the order of the growth rate obtained from the evaporation-wind feedback alone.

The system (11) contains other modes which have nonzero v that are related to the usual shallow water Rossby, gravity and Rossby–gravity modes when m is nonzero. Using the longwave approximation (u is geostrophic balance) to select the Rossby-related modes, one finds them to be damped by the evaporation-feedback mechanism when the basic state flow is easterly ($A > 0$). It does not seem fruitful to examine these in detail.

4. GCM experiments

The effects of the evaporation–wind feedback can be very cleanly tested in a general circulation model: the feedback can be explicitly suppressed without affecting the time-mean climatology significantly. Unfortunately, there is no such direct way of testing the hypothesized effects of the moist static stability, but we perform further experiments using lower boundary conditions that disfavor the evaporation–wind feedback and attempt to make some inferences from these. All calculations were carried out using a spectral model with rhomboidal truncation at wavenumber 15 (R15) constructed at GFDL (Manabe and Hahn, 1981; Gordon and Stern, 1982). This model has an analog to the 30–50 day wave when realistic land–sea boundary conditions are used, although the phase speed, ≈ 15 m s^{-1}, is faster than is observed (Lau and Lau, 1986). An R30 model produces somewhat lower-frequency oscillations (Hayashi and Golder, 1986). To construct an idealized model, we remove continents from the R15 GCM and force the model with annual mean insolation. Surface albedos are set equal to 0.1 everywhere and clouds are prescribed as a function of latitude only, symmetric about the equator. Moist convection is simulated with the convective adjustment scheme of Manabe et al. (1965).

Two pairs of experiments are performed. Model statistics are computed from 1400 days of integration in each case, discarding a spinup period of 200–400 days. The experiments are referred to as 1) "fixed SST", 2) "fixed SST − fixed V", 3) "swamp", 4) "swamp − fixed V". The first pair tests the effect of the evaporation–wind feedback. In the second pair, the lower boundary condition is chosen to disfavor processes that involve energy exchange with the lower boundary, including the evaporation–wind feedback. The nature of low-frequency variability in the absence of such exchanges can then be examined.

1) "fixed SST": We think of this as the control run since the tropics are primarily ocean-covered. The prescribed sea surface temperatures are zonally symmetric as well as symmetric about the equator. To facilitate intercomparison of the calculations, the fixed surface temperature profile is derived from the climatological surface temperature generated by experiment 3. This surface temperature has a value of 304 K at a broad maximum about the equator.

2) "fixed SST − fixed V": This case is identical to experiment 1 except that the evaporation-wind feedback mechanism is eliminated by modifying the GCM evaporation parameterization to remove the dependence on wind speed. The time-varying wind speed in (9) is replaced by a time-mean wind speed that is a function only of latitude and is symmetric about the equator. Its value at the equator is 6 m s^{-1}. The time-mean evaporation fields in experiments 1 and 2 are nearly identical. The sensible heat parameterization is modified in the same manner since it could produce a similar, though weaker feedback.

3) "Swamp": The lower boundary resembles a saturated land surface in that the heat capacity is zero and the surface has an infinite supply of moisture. These conditions are of interest both because they are appropriate over moist tropical continents and because this boundary condition should act to suppress or change the evaporation–wind feedback. With this boundary condition, the net energy flux into the surface is required to be zero at each instant, so an increase in evaporation due to higher wind speed must be balanced by other components in the surface energy budget. Changes in the longwave flux emitted from the surface dominate the adjustment since sensible heat tends to increase along with the evaporation when the wind speed increases, while the incoming shortwave is approximately constant in this model with prescribed clouds. Since the longwave radiation is largely absorbed in the atmosphere, an additional term must be added

to (3) that will cancel the evaporation anomaly when the terms are combined in (11c). In a model with more than one temperature level, differences in vertical structure between the latent, sensible and radiative heating might permit some effect of the evaporation anomaly even with swamp boundary conditions, but one suspects the attributes of any mode that depends on the evaporative feedback to be substantially changed.

4) "Swamp − fixed V": Swamp boundary conditions are combined with the removal of the wind speed dependence in the evaporation and sensible heating.

The low-frequency variability in the tropics of these four runs is compared in Figs. 1–4, which show the frequency spectra of the zonal wind field along the equator at 205 and 940 mb for zonal wavenumbers 1 and 2. Winds are averaged over the two grid points at ±2.25° latitude. The variance is divided into eastward- and westward-moving components and a tapered band average of halfwidth 0.011 cycles per day (cpd) is used in computing the spectra. A half-cosine tapering of the first and last 10% of the time series is applied prior to calculation of the Fourier coefficients. In each case, the full time series is divided into two 700-day parts and spectra for each half are shown in the figures to provide an estimate of the reproducibility of the spectra. In general, the spectra are more reproducible at lower levels than at upper levels, probably because very low-frequency disturbances generated by midlatitude dynamics do not penetrate the mean easterlies at low levels, while they do contaminate the flow at upper levels in the tropics.

What we believe to be the model's analog of the 30–50 day oscillation may be seen in the fixed SST control calculation as peaks in eastward propagating power in wavenumber 1 at 20–27 day period, and 12–15 day in wavenumber 2. Note the clear indication that this oscillation is characterized by a phase speed roughly independent of k, rather than by a particular frequency. The phase speed is about 20 m s^{-1}. In the control run, the peak at this phase speed contains a considerable fraction of the total power in the wavenumber 1 component of the zonal wind—at 940 mb, the portion of the eastward-propagating peak between 48 and 15 days contains 44% of the total variance with period greater than two days. One obvious conclusion is that the GCM analog of the 30–50 day oscillation does not depend on zonal asymmetry in any fundamental way.

The comparison between experiments 1 and 2 tests the evaporation–wind feedback mechanism (parts a and b of the figures). In all four figures there is a very marked reduction in the amplitude of the spectral peak in the fixed V experiment. However, the oscillation does not disappear completely; there is unquestionably still more power in eastward than in westward propagating waves. Since the peaks do not stand out as distinctly from the background noise in the fixed V case, it is difficult to determine whether there has been a shift in the dominant frequency. Similar results are found in spectra of other fields, such as surface pressure.

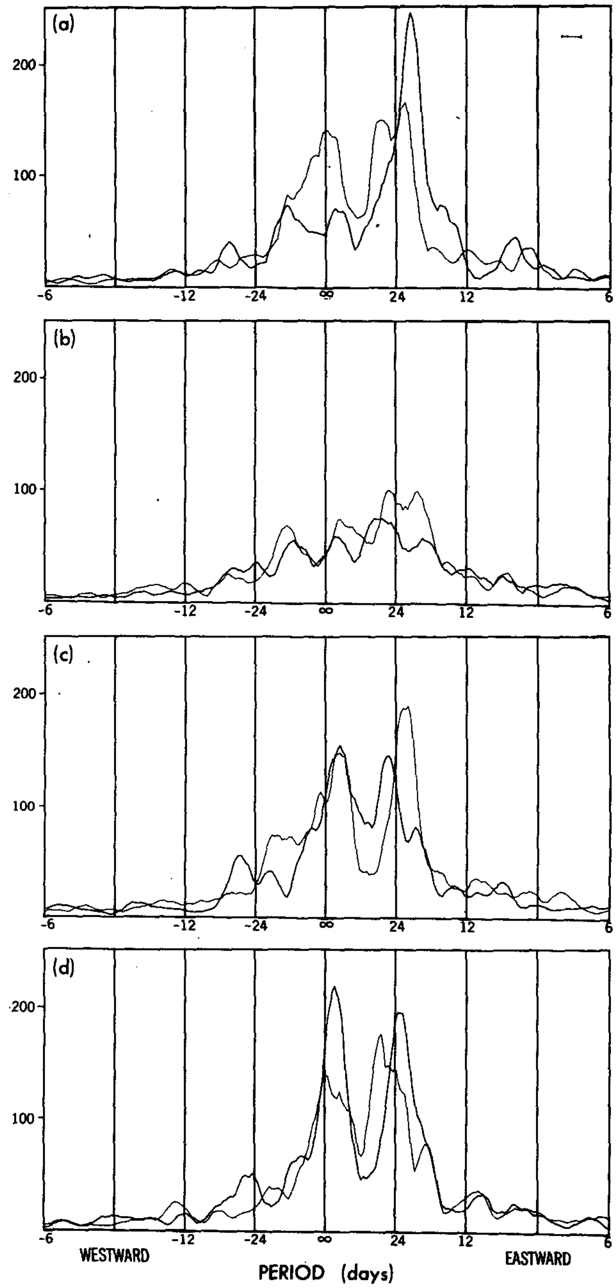

FIG. 1. Variance spectra of 205-mb u along the equator for zonal wavenumber 1: (a) fixed SST (control) run, (b) fixed SST − fixed V run, (c) swamp run, (d) swamp − fixed V run. Light and heavy solid lines represent the spectra of the first and second 700 days of each run, respectively. The lowest frequency resolved is 1/700 cpd. Negative frequencies denote westward-propagating variance. The bandwidth, 0.011 cpd, is indicated in the upper right corner. The vertical scale is linear with a maximum value of 252 m^2 s^{-2} day.

This result speaks strongly for the importance of the evaporation–wind feedback mechanism. If only this

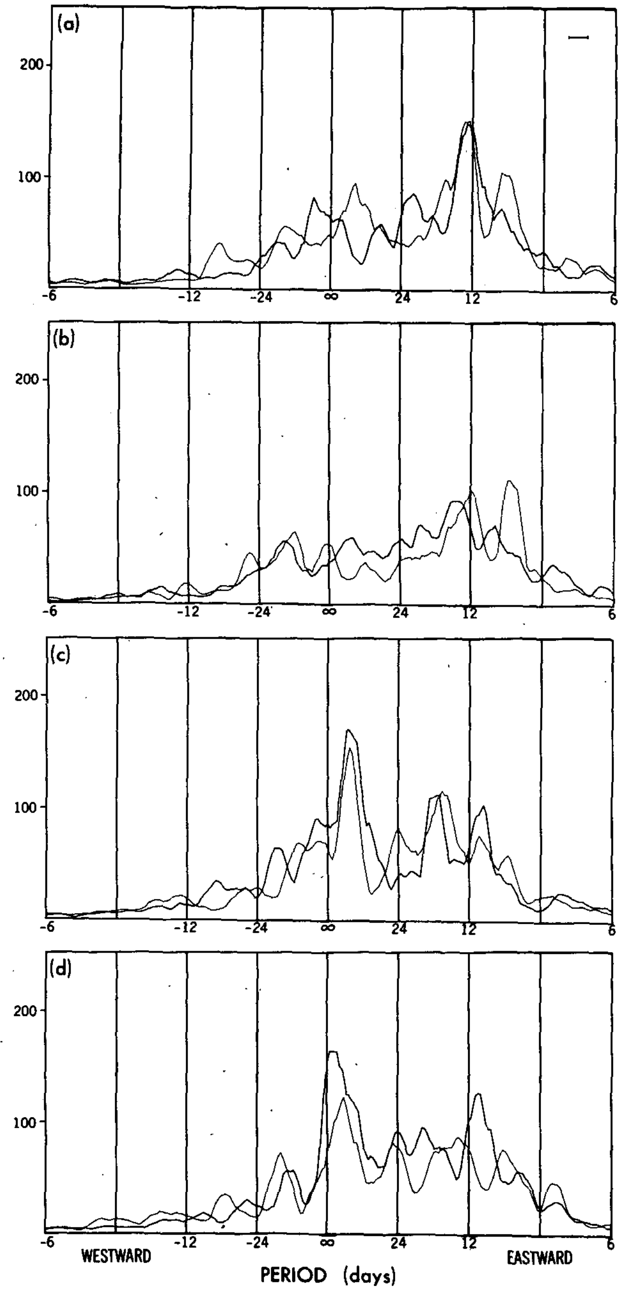

FIG. 2. As in Fig. 1, but zonal wavenumber 2.

first pair of experiments had been performed, one might be tempted to conclude that the evaporation–wind feedback mechanism was almost solely responsible for the 30–50 day oscillation. However, examination of a second pair (the swamp runs) suggestes that the sources of low-frequency variability are more complex. While the swamp boundary condition should act to suppress or modify the effects of the evaporation-wind feedback, in fact there are quite distinct peaks in the swamp run at similar frequencies to those in the control run. The peaks are less distinct in the 940 mb u spectra than at 205 mb, but compositing techniques show a low-level wind pattern similar to the upper-level winds, opposite in sign and smaller in magnitude (N. C. Lau, personal communication). The composites also suggest that the structure of this mode is generally similar to that of the corresponding mode in the fixed SST experiment and in the GCM with realistic boundary conditions described by Lau and Lau (1986).

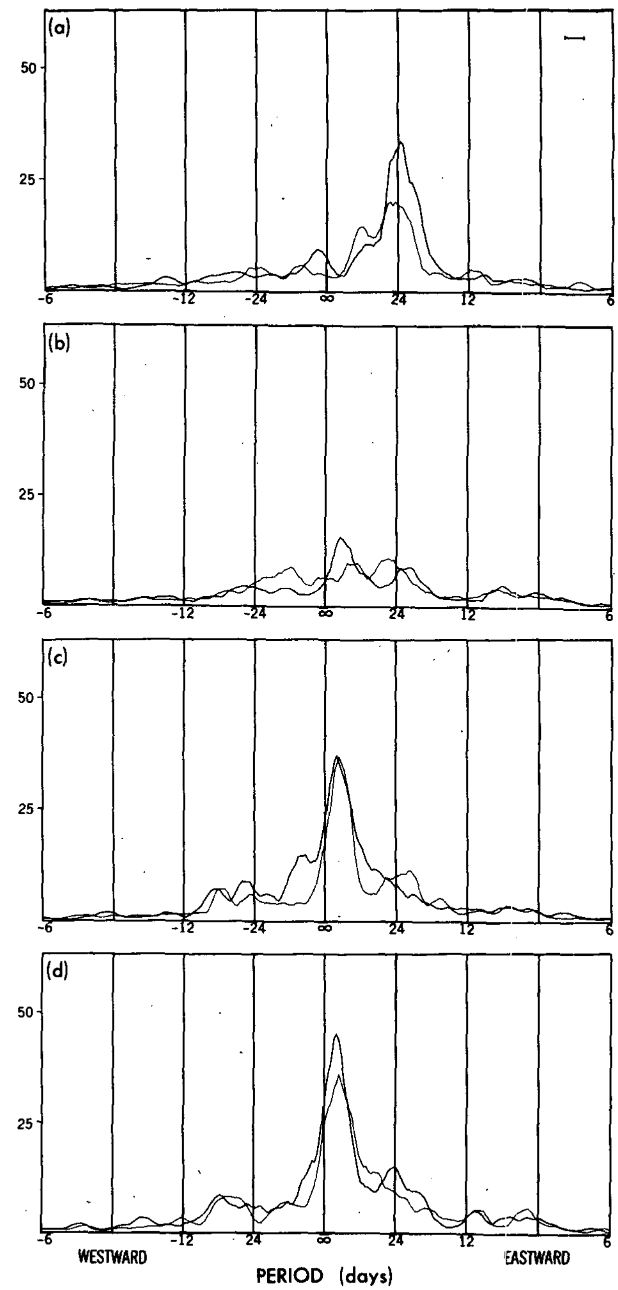

FIG. 3. As in Fig. 1, but for u at 940 mb, wavenumber 1. The vertical scale is one quarter that of Fig. 1.

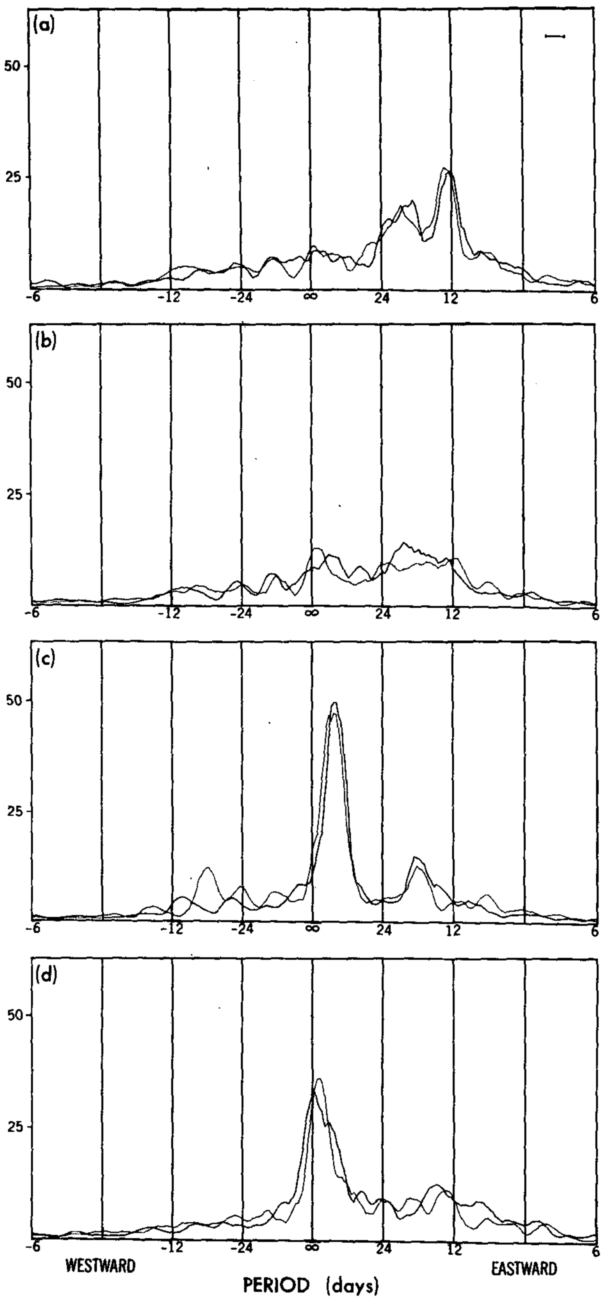

FIG. 4. As for Fig. 3, but for wavenumber 2.

There are also very strong and highly reproducible peaks in the spectra of the swamp model at the remarkably long periods of about 120 days for wavenumber 1, and 70 days for wavenumber 2. The corresponding phase speed is roughly 3 m s^{-1}. Compositing indicates that this mode is similar to the 24-day mode in having equatorial latent heating with associated baroclinic wind patterns, but it has a larger temperature perturbation at the surface. The characteristics of this mode and of the 24-day mode seen in these experiments will be described elsewhere in more detail.

We expect the evaporation–wind feedback *not* to be important in the swamp run, and the comparison to the swamp − fixed V run shows this to be true; one finds little difference in the spectra. The changes in the 24- and 10–15-day peaks are smaller than the differences between the two halves of each time series. In short, this mode of variability is not suppressed when the evaporation–wind feedback is explicitly removed in the presence of swamp boundary conditions. There are some changes in the very low-frequency mode. The amplitude of the 70-day peak in u at 940 mb for wavenumber 2 is considerably reduced in the fixed V case, although it is by no means entirely suppressed, and at 205 mb the very low-frequency peaks are less well defined and have shifted toward lower frequencies. The fact that this very low-frequency peak is quite reproducible in the swamp run, particularly at the lower level, lends some credibility to these changes. However, the amplitude of the wavenumber 1 very low-frequency peak is not reduced.

5. Conclusions

The evaporation–wind feedback has some appeal as a mechanism for generating the 30–50 day oscillation since it produces an eastward-propagating, equatorially trapped mode with low phase speed that is approximately independent of k for low wavenumbers. In addition, it can produce growth rates that overcome the strong damping which exists in the lower troposphere. The growth of the wave is supported by drawing energy from the fixed surface temperature lower boundary. The hypothesis has been directly tested in a GCM by removing the wind speed dependence in the parameterizations of evaporation and sensible heating. When fixed SST lower boundary conditions are used, the result is a dramatic reduction in the amplitude of the spectral peaks which we believe are the analog of the 30–50 day oscillation in the GCM.

However, the suppression of the evaporation–wind feedback does not entirely remove the preponderance of eastward over westward moving low-frequency waves at the equator. This raises the question of whether other mechanisms may be active. Within the context of the two-layer model presented here, the evaporation–wind feedback can coexist (in the same mode) with a second mechanism for producing low-frequency, eastward-propagating waves in the tropics. Without the feedback, the system has a conventional equatorial Kelvin wave, but with a phase speed that depends on an effective moist static stability Δm instead of a dry static stability Δs. If Δm is sufficiently small compared to Δs, this can potentially give "moist Kelvin wave" speeds of the right magnitude, although accurate estimation of the parameter Δm is difficult. When both nonzero Δm and the evaporation–wind feedback are present, a hybrid mode is destabilized by the feedback mechanism.

A further pair of experiments is performed using swamp lower boundary conditions. In this case, processes involving exchange of energy with the lower boundary, including the evaporation–wind feedback, and disfavored. Spectral peaks of a similar frequency to those in the fixed SST case are found and, as expected, the evaporation–wind feedback is not important for their maintenance. While the fixed SST case is much more realistic than the swamp case since the tropics are primarily ocean covered, the results of the swamp run are useful in illustrating that the evaporation–wind feedback is not the only mechanism which contributes to the low-frequency variability in the tropics. We interpret the oscillation in the swamp model as being associated with the moist static stability. This interpretation is consistent with the reduction in power, but not complete suppression, of the low-frequency, eastward-propagating oscillations when the evaporation–wind feedback is removed from the fixed SST GCM; the evaporation–wind feedback is apparently very important in maintaining the hybrid wave, but even without the feedback some vestige of the oscillation remains, perhaps excited by low-frequency noise. We speculate that in the swamp case the wave is less strongly damped and thus not dependent on the evaporation–wind feedback for its maintenance. The effective damping should be stronger in the fixed SST case; in the absence of the evaporation–wind feedback, one expects the fixed temperature lower boundary to act as an energy sink for the oscillation.

Unfortunately, we have been unable to test the moist static stability hypothesis by intervening directly in the GCM, as with the evaporation–wind feedback, because it involves a complex interaction between the convective parameterization and the dynamics. Neither have we been able to obtain a suitable estimate of Δm directly from the moist static energy budget of the GCM. Future work will address these issues.

The experiments with swamp lower boundary conditions also contain a remarkable very low frequency mode of period about 120 days for wavenumber 1. Removal of the evaporation–wind feedback has some effect on this mode, but not a dramatic one. We have no explanation for this mode's existence at present, an indication of current limitations in understanding low-frequency variability in the tropical atmosphere, and, for that matter, in the tropics of idealized general circulation models.

Acknowledgments. We are especially grateful to N. C. Lau and T. R. Knutson for access to unpublished diagnostics of the low-frequency variability of the GCM. We also thank N. C. Lau and B. Wang for helpful comments on the manuscript and R. T. Pierrehumbert and Y. Hayashi for useful discussions. One of the authors (JDN) was supported by a postgraduate scholarship from the Natural Sciences and Engineering Research Council of Canada.

REFERENCES

Chang, C. P., 1977: Viscous internal gravity waves and low-frequency oscillation in the tropics. *J. Atmos. Sci.*, **34**, 981–991.

Emanuel, K. A., 1987: An air–sea interaction model of intraseasonal oscillations in the tropics. *J. Atmos. Sci.*, **44**, 2224–2240.

Gill, A. E., 1980: Some simple solutions for heat-induced tropical circulation. *Quart. J. Roy. Meteor. Soc.*, **106**, 447–462.

Gordon, C. T., and W. F. Stern, 1982: A description of the GFDL global spectral model. *Mon. Wea. Rev.*, **110**, 625–644.

Goswami, B. N., and J. Shukla, 1984: Quasi-periodic oscillations in a symmetric general circulation model. *J. Atmos. Sci.*, **41**, 20–37.

Hayashi, Y., and D. Golder, 1986: Tropical intraseasonal oscillations appearing in a GFDL GCM and FGGE data. Part I: Phase propagation. *J. Atmos. Sci.*, **43**, 3058–3067.

Hayashi, Y. Y., and A. Sumi, 1986: The 20–40-day oscillation simulated in an "aqua-planet" model. *J. Meteor. Soc. Japan*, **64**, 451–466.

Krishnamurti, T. N., P. K. Jayakumar, J. Sheng, N. Surgi and A. Kumar, 1985: Divergent circulations on the 30- to 50-day time scale. *J. Atmos. Sci.*, **42**, 364–375.

Lau, K. M., and P. H. Chan, 1985: Aspects of the 40–50-day oscillation during northern winter as inferred from outgoing longwave radiation. *Mon. Wea. Rev.*, **113**, 1889–1909.

——, and L. Peng, 1987: Origin of low-frequency (intraseasonal) oscillations in the tropical atmosphere. Part I: The basic theory. Submitted to *J. Atmos. Sci.*

Lau, N. C., and K. M. Lau, 1986: The structure and propagation of intraseasonal oscillations appearing in a GFDL GCM. *J. Atmos. Sci.*, **43**, 2023–2047.

Lindzen, R. S., 1974: Wave-CISK in the tropics. *J. Atmos. Sci.*, **31**, 156–179.

Lorenc, A. C., 1984: The evolution of planetary scale 200 mb divergences during the FGGE year. *Quart. J. Roy. Meteor. Soc.*, **110**, 427–442.

Madden, R., and P. R. Julian, 1971: Detection of a 40–50 day oscillation in the zonal wind in the tropical Pacific. *J. Atmos. Sci.*, **28**, 702–708.

——, and ——, 1972: Description of global-scale circulation cells in the tropics with a 40–50 day period. *J. Atmos. Sci.*, **29**, 1109–1123.

Manabe, S., and D. G. Hahn, 1981: Simulation of atmospheric variability. *Mon. Wea. Rev.*, **109**, 2260–2286.

——, J. Smagorinsky and R. F. Strickler, 1965: Simulated climatology of a general circulation model with a hydrological cycle. *Mon. Wea. Rev.*, **93**, 769–798.

Maruyama, T., 1982: Upper tropospheric zonal wind oscillation with a 30–50 day period over the equatorial western Pacific observed in cloud movement vectors. *J. Meteor. Soc. Japan.*, **60**, 172–181.

Matsuno, T., 1966: Quasi-geostrophic motions in the equatorial area. *J. Meteor. Soc. Japan.*, **44**, 25–42.

Murakami, T., and T. Nakazawa, 1985: Tropical 45-day oscillations during the 1979 Northern Hemisphere summer. *J. Atmos. Sci.*, **42**, 1107–1122.

Neelin, J. D., and I. M. Held, 1987: Modeling tropical convergence based on the moist static energy budget. *Mon. Wea. Rev.*, **115**, 3–12.

Stevens, D. E., 1983: On symmetric instability and instability of zonal mean flows near the equator. *J. Atmos. Sci.*, **40**, 882–893.

Sui, C.-H., and M. Yanai, 1986: Cumulus ensemble effects on the large-scale vorticity and momentum fields of GATE. Part I: Observational evidence. *J. Atmos. Sci.*, **43**, 1618–1642.

Webster, P. J., 1983: Mechanisms of monsoon low-frequency variability: Surface hydrological effects. *J. Atmos. Sci.*, **40**, 2110–2124.

Yamagata, T., and Y. Hayashi, 1984: A simple diagnostic model for the 30–50-day oscillation in the tropics. *J. Meteor. Soc. Japan.*, **62**, 709–717.